修士論文要旨 (2017 年度)

厚みのある導体スリットによるH偏波の平面波回折

H Polarized Plane Wave Diffraction by Thick Conducting Slits

電気電子情報通信工学専攻　ヌェン ナム カーン
Nguyen Nam Khanh

1. Introduction

Outdoor-indoor wireless communication has been paid attention because of its important role in seeking reliable channels for recent connection demand. A primary gate for such outdoor-indoor propagation could be windows on building walls, since the signal decays rapidly as it passes through the concrete walls, especially as the frequency increases. Accordingly, it is essential to analyze the scattering features of the window.

Classical problem for such aperture diffraction is the analysis of plane wave diffraction by a slit perforated on a conducting screen. A slit on an infinitely thin screen has been considered by Morse and Rubinstein using an eigenfunction expansion solution in terms of Mathieu functions [1], and by Nomura and Katsura using Kobayashi Potential (KP) method with Weber-Schafheitlin discontinuous integrals [2]. KP method can also be utilized to solved thick slit problems [3], [4] which are more complicated than the thin slit case. However, the above results have mainly considered relatively narrow slit apertures.

Since scattering by a window whose large dimension compared with the wavelength should be formulated to consider a practical wireless communication situation, I focus on the study of wide slit rather than narrow one. For this case, it would be better to apply high-frequency asymptotic method, such as the Geometrical Theory of Diffraction (GTD) [5],[6] and Kirchhoff approximation [7], rather than eigenfunction expansion method [2, 3, 4],[8] which is known to give a reliable result for relatively narrow aperture case. Besides, using GTD method to derive diffraction coefficient of the local scattering feature, difficulties arise in the derivation of the appropriate coefficients for the corners or dielectric wedge diffraction. Therefore, in Sect. 2, Kirchhoff approximation is applied to formulate the scattering far-field, and the accuracy assessment should be done for the case which the other solutions are available. In the formulation, the field propagating in the slit could be calculated in terms of waveguide modes excited at the aperture of the slit. Some numerical calculations are performed and comparisons with other solutions to validate the analysis are given in Sect. 3 with some concluding remarks.

Time harmonic factor $e^{-i\omega t}$ is assumed and suppressed throughout the context.

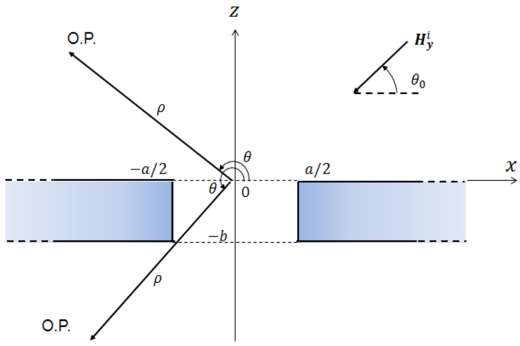

Figure 1: Geometry of the problem.

2. Formulation

As illustrated in Fig. 1, an H-polarized plane wave:

$$H_y^i = H_0 e^{-ik(x\cos\theta_0 + z\sin\theta_0)} \tag{1}$$

impinges upon a slit perforated on an infinitely long perfectly conducting thick screen with incident angle θ_0. The width and thickness of the slit are a and b, respectively, and k is free space wavenumber. In order to obtain the scattering contribution, the aperture integration method is utilized. By this method, the scattering fields are derived as radiations from the equivalent sources on the virtually closed aperture.

2.1 Scattering in the upper region

On the upper half-space ($z > 0$), there exists a reflected field $\boldsymbol{H}^r$ due to the reflection from the screen's surface at $z = 0$. This contribution will be omitted in the following analysis. The equivalent magnetic current sources $\boldsymbol{M}_1^{\pm}$ on the closed upper aperture may be obtained from the incident electric field as

$$\boldsymbol{M}_1^{\pm}(x, z=0) = \left(E_x^i \hat{\boldsymbol{x}} + E_z^i \hat{\boldsymbol{z}}\right)\Big|_{z=0} \times (\pm\hat{\boldsymbol{z}}), \tag{2}$$

where '^' denotes the corresponding unit vector. Then scattering H_{1y}^s field from the upper aperture can be expressed in terms of the equivalent magnetic current $\boldsymbol{M}_1^+$ on the upper side of upper aperture as

$$H_{1y}^s = i\omega\varepsilon_0 \int_{-a/2}^{a/2} M_{1y}^+(x')G dx', \tag{3}$$

where ε_0 denotes the free space permittivity, G is the half-space 2D Green's function, considering the imaging

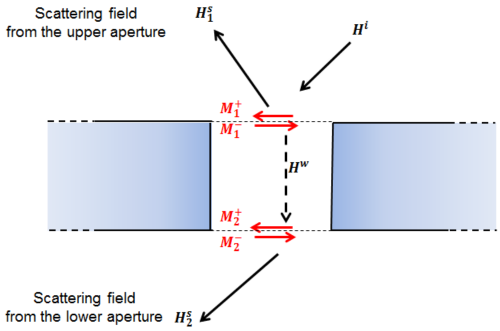

Figure 2: Scattering field at each region may be considered as radiation from the equivalent sources at the apertures.

effect of the magnetic current on the boundary

$$G = \frac{i}{2}\mathrm{H}_0^{(1)}(k\sqrt{(x-x')^2+(z-z')^2}) = \frac{i}{2\pi}\int_{-\infty}^{\infty}\frac{e^{i\eta(x-x')+i\sqrt{k^2-\eta^2}|z-z'|}}{\sqrt{k^2-\eta^2}}d\eta. \quad (4)$$

Substituting Eq.(4) into (3) and evaluating the integral with respect to x' variable first, the saddle point method may be applied to evaluate the integral with respect to η variable on the assumption for large k, one can derive the scattering far-field at the upper half-space ($z > 0$) as

$$H_{1y}^s = \frac{4iH_0\sin\theta_0\sin\left\{\frac{ka}{2}(\cos\theta_0+\cos\theta)\right\}}{\cos\theta_0+\cos\theta}C(k\rho), \quad (5)$$

$$C(k\rho) = \sqrt{\frac{1}{8\pi k\rho}}e^{ik\rho+i\frac{\pi}{4}}, \quad (6)$$

where $C(k\rho)$ is an asymptotic far-field form of Eq.(4).

2.2 Modal excitation inside the slit

A part of the incident plane wave impinges the slit aperture. According to the Kirchhoff approximation, the field inside the slit can be excited by the equivalent magnetic source $\boldsymbol{M}_1^-$ in Eq.(2) on the closed aperture. The field $\boldsymbol{H}^w$ inside a semi-infinitely long ($b \to \infty$) parallel plane waveguide may be expressed as

$$H_y^w = i\omega\varepsilon_0\int_{-a/2}^{a/2}M_{1y}^-(x')G^w dx', \quad (7)$$

where G^w is the Green's function for parallel plane waveguide considering the imaging effect for the metal closure at the aperture, namely

$$G^w(x,z;x',z') = \sum_{m=0}^{\infty}\frac{i\epsilon_m}{a\zeta_m}\cos\frac{m\pi}{a}\left(x+\frac{a}{2}\right) \cdot \cos\frac{m\pi}{a}\left(x'+\frac{a}{2}\right)e^{i\zeta_m|z-z'|}, \quad (8)$$

where

$$\epsilon_m = \begin{cases}1, & m=0\\ 2, & m>0\end{cases}, \quad \zeta_m = \sqrt{k^2-\left(\frac{m\pi}{a}\right)^2}. \quad (9)$$

It is found that the field propagating downward inside the slit could be derived as

$$H_y^w = \sum_{m=0}^{\infty}F_m\cos\frac{m\pi}{a}\left(x+\frac{a}{2}\right)e^{-i\zeta_m z}. \quad (10)$$

Here, F_m is the excitation coefficient of the $\mathrm{TM_m}$ waveguide modal field. F_m can be calculated by integrating the equivalent source $\boldsymbol{M}_1^-$ over the aperture ($|x| \le a/2, z=0$), one gets

$$F_m = -\frac{i\epsilon_m k^2 aH_0\sin\theta_0\cos\theta_0}{\zeta_m\{(m\pi)^2-(ka\cos\theta_0)^2\}} \cdot\left\{(-1)^m\cdot e^{(-ika\cos\theta_0)/2}-e^{(ika\cos\theta_0)/2}\right\}. \quad (11)$$

The internal waveguide field $\boldsymbol{H}^w$ propagates down to the lower aperture ($z=-b$) and excites there scattering field $\boldsymbol{H}_2^s$ to the lower half-space ($z<-b$), and the modal reflection ($z>-b$). These scattering fields are again calculated from the equivalent magnetic currents $\boldsymbol{M}_2^\pm$ on the closed aperture at $z=-b$, as in Fig. 2, as

$$\boldsymbol{M}_2^\pm(x,z=-b) = (E_x^w\hat{\boldsymbol{x}}+E_z^w\hat{\boldsymbol{z}})\big|_{z=-b}\times(\pm\hat{\boldsymbol{z}}). \quad (12)$$

For modal reflection, one may use the similar formula in Eq.(7) with M_{2y}^+ in Eq.(12). After some calculation, one may find that there is no reflection at all for the Kirchhoff approximation. In the previous formulation by GTD [6], there is at least modal reflection and coupling even at the lower aperture, while these effects are weak.

2.3 Scattering in the lower region

The radiation field $\boldsymbol{H}_2^s$ in the lower half-space can be derived from the equivalent source $\boldsymbol{M}_2^-$ in Eq.(12) like the primary scattering field $\boldsymbol{H}_1^s$ in Sect. 2.1. Once again, the integral in this formulation can be evaluated using the saddle point method. Finally, one gets the scattering field $\boldsymbol{H}_2^s$ as

$$H_{2y}^s = 2iH_0(ka)^3\sin\theta_0\cos\theta_0\cos\theta\cdot C(k\rho) \cdot\sum_{m=0}^{\infty}\frac{\epsilon_m}{\{(m\pi)^2-(ka\cos\theta_0)^2\}\{(m\pi)^2-(ka\cos\theta)^2\}} \cdot\left\{(-1)^m e^{(-ika\cos\theta_0)/2}-e^{(ika\cos\theta_0)/2}\right\} \cdot\left\{(-1)^m e^{(-ika\cos\theta)/2}-e^{(ika\cos\theta)/2}\right\} \cdot e^{i\zeta_m b}. \quad (13)$$

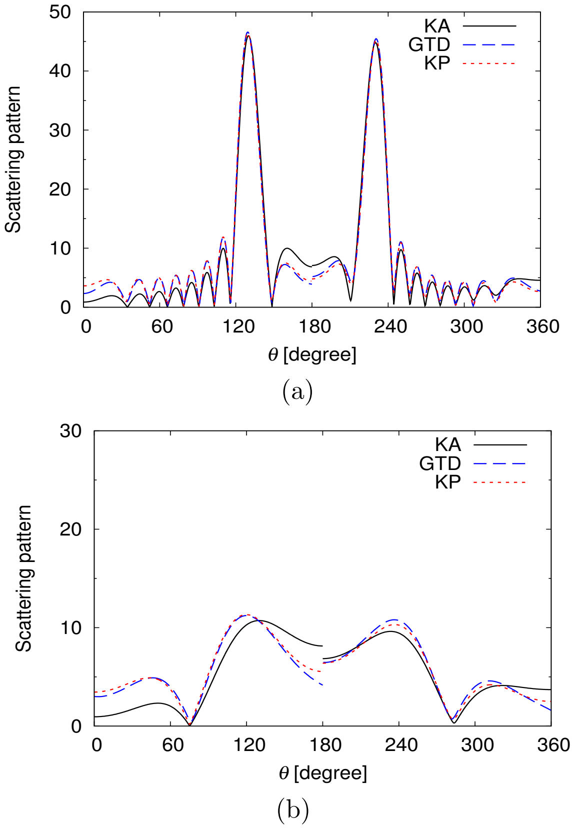

Figure 3: Comparison of the far-field patterns (width variation) of KA, KP [3], and GTD [6] methods . $\theta_0 = 50°$, $kb = 2$. (a) $ka = 30$. (b) $ka = 7$.

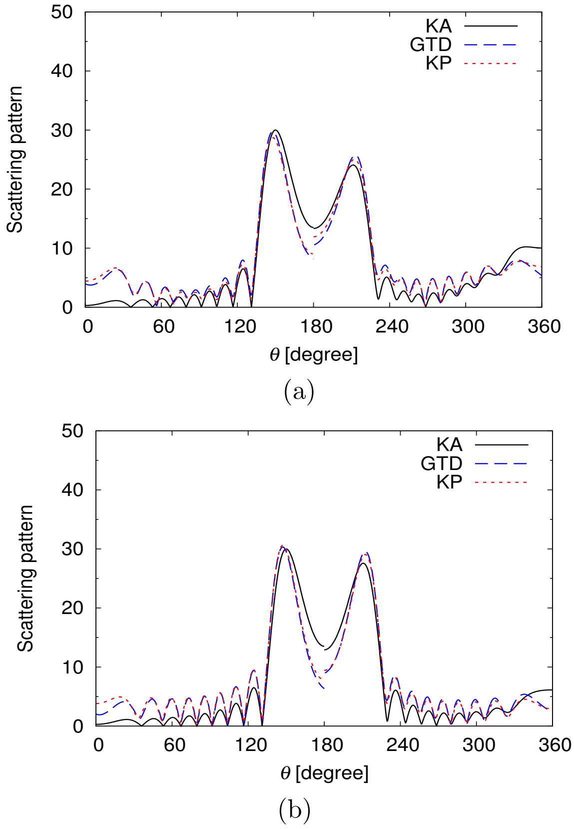

Figure 4: Comparison of the far-field patterns (thickness variation) of KA, KP [3] and GTD [6] methods. $\theta_0 = 30°$, $ka = 30$. (a) $kb = 4$. (b) $kb = 2$.

3. Numerical results and discussion

I first check the validity of the presented solution by comparing the numerical results with those obtained from other methods. In the following calculation, a common factor $C(k\rho)$ is omitted. In the upper half-space ($z > 0$), the reflected plane wave exists but is omitted as mentioned in Sect. 2. Fig. 3 shows the effect of the aperture width. Fig. 3(a) is for a wide case ($ka = 30$), while Fig. 3(b) for a narrow case ($ka = 7$). The figures include results obtained from the KP [3] and GTD [6] methods. GTD method is known to give us accurate results for large aperture case [6], while KP method is believed to yield the accuracy of narrow aperture case [3]. Thickness b of the slit and the incident angle θ_0 are set as $kb = 2$ and $50°$, respectively. It is found that good agreement among the present KA and the other results for the observation angles of the main beam. Though the multiple edge-diffractions between the edges are not considered in this calculation, the result matches well even for narrow aperture case in Fig. 3(b). Scattering pattern is almost symmetric with respect to the x-axis (screen) in this thickness condition.

Next, I shall check the accuracy of the thickness variation of the slit. Fig. 4 shows the far-field patterns for relatively thick ($kb = 4$) and thin ($kb = 2$) cases. Here, the width of the slit a and the incident angle θ_0 are chosen as 4.47λ ($ka = 30$) and $30°$, respectively. From these results, the solution is in good agreement with the references for both thickness cases.

While the presented formulation is based on the thick screen, it may be interesting to take a limit case of zero thickness. Fig. 5 shows a comparison of the scattering patterns for the infinitely thin case. As reference solutions, the case for a very thin screen is calculated by KA and KP. One can notice slight differences mainly at the screen boundary direction ($\theta = 0°, 180°, 360°$).

Fig. 6(a) and (b) show the scattering pattern change due to the screen thickness. In the upper half-space, the field $\boldsymbol{H}_1^s$ which is described in Eq. (5) gives scattering pattern feature. As can be seen from the equation, the scattering value does not depend on the thickness value b, so that the scattering pattern does not change as the thickness varies. On the other hand, the pattern changes in diffraction range (lower half-space). The dependence of the scattering $\boldsymbol{H}_2^s$ field value on the thickness value b is described in Eq. (13). When the screen is thin, the

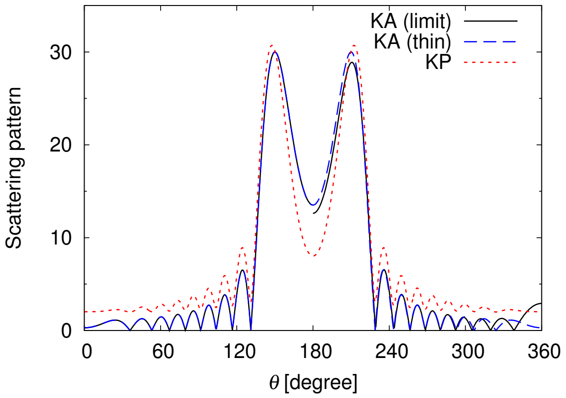

Figure 5: Comparison of the far-field patterns in thin slit case. $\theta_0 = 30°$, $ka = 30$, $kb \to 0$.

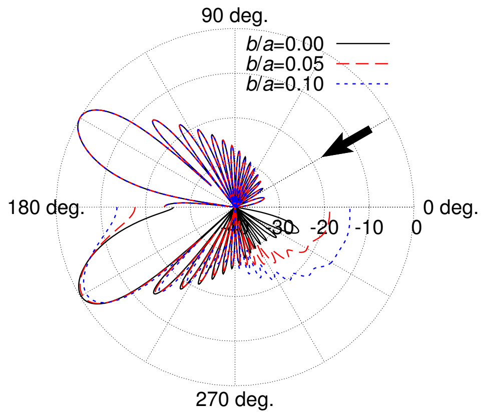

(a)

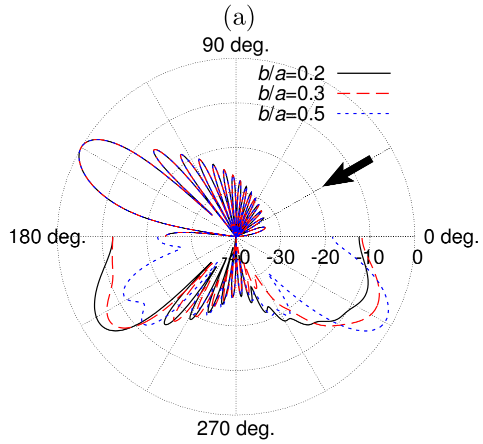

(b)

Figure 6: Change of normalized far-field patterns in dB. $\theta_0 = 30°$, $ka = 50$. (a) $kb = 0, 2.5, 5$. (b) $kb = 10, 15, 25$.

incident beam truncated by aperture transmits to the forward direction ($\theta = \theta_0 + \pi$). As the screen gets thicken, the truncated beam experiences its thickness, and beam split occurs. For the case of the incident angle $\theta_0 = 30°$ and the ratio of thickness and aperture width $b/a = 0.5$, main of the truncated beam reflects at slit's internal wall and propagates to the direction at $\theta = 330°$, as in Fig. 6(b). One may also conclude that the scattering pattern can be predicted by a simple half plane solution if the thickness of the screen is less than 0.5λ.

Acknowledgment

I appreciated greatly that MEXT and Chuo University have provided me great opportunity to study in Japan. I would also like to take this opportunity to express my gratitude to Prof. Hiroshi Shirai for his supervision of this research. And this work has been supported partially by from JSPS Grant.

References

[1] P. M. Morse and P. J. Rubenstein, "The diffraction of waves by ribbons and by slits," *Phys. Rev.*, vol. 54, no. 11, pp. 895–898, 1938.

[2] Y. Nomura and S. Katsura, "Diffraction of electromagnetic waves by ribbon and slit. I," *J. Phys. Soc. Jpn.*, vol. 12, no. 2, pp. 190–200, 1957.

[3] K. Hongo, "Diffraction of electromagnetic plane wave by infinite slit perforated in a conducting screen with finite thickness," *Trans. IECE*, vol. 54B, no. 7, pp. 419–425, Jul. 1971 (in Japanese).

[4] K. Hongo and G. Ishii, "Diffraction of an electromagnetic plane wave by a thick slit," *IEEE Trans. Antennas Propag.*, vol. 26, no.3, pp. 494–499, May 1978.

[5] S. N. Karp and A. Russek, "Diffraction by a wide slit," *J. Appl. Phys.*, vol. 27, no. 8, pp. 886–894, Aug. 1956.

[6] H. Shirai and R. Sato, "High frequency ray-mode coupling analysis of plane wave diffraction by a wide and thick slit on a conducting screen," *IEICE Trans. Electron.*, vol. E95-C, no. 1, pp. 10–15, Jan. 2012.

[7] K. N. Nguyen and H. Shirai, "Electromagnetic plane wave scattering by a rectangular hole in a thick conducting screen," *Proc. of 2017 International Conference on Electromagnetics and Advanced Applications*, CDROM, Sep. 2017.

[8] H. Serizawa, "Diffraction of a plane wave by a rectangular hole in a thick conducting screen," *Proc. of 2015 European Conference on Antennas and Propagation*, pp. 1–5, Apr. 2015.